Radiative heating rates profiles associated with a springtime case of Bodélé and Sudan dust transport over West Africa

Author(s): C. Lemaître et al.
MS No.: acp-2010-86

Reply to the Referee 2

We thank the reviewer for his/her helpful corrections and thoughtful suggestions on our previously submitted manuscript. All comments have been taken into account when producing the revised manuscript.

1. *Limitation of data duration:* In this study we detail the method to derive dust-related heating rate profiles and analyse their spatial variability using a very comprehensive dataset that is only available on 13 and 14 June 2006. One important aspect of this work is to show that reliable heating rates can be retrieved from the space-borne lidar CALIOP. As a result, dust-related heating rates can be obtained across West Africa for much longer periods of time. This work was done for the entire 9-15 June episode but was not included in the present study because it is already quite extensive. Nevertheless, CALIOP data for that period evidence that the results presented in this paper regarding the daytime/nighttime structure of heating rate profiles are representative of the entire 9-15 June episode.

2. *Assumption of externally mixes aerosol*: Aerosol single scattering albedo, asymmetry factor and extinction coefficient at several wavelength are based on the synergetic use of observations from lidar, radiometry and in situ airborne measurements as in Raut and Chazette (2008). This determination is based on optical measurements so no assumptions on the type of mixture (external or internal) are necessary.

3. *Errors resulting from non-spherical shape of dust aerosol*: We have conducted a study in which the aerosols are modelled as non spherical shapes rather than spherical particles. No significant differences were found between the results from the Mie model with spherical particles and Mishchenko T-matrix code (Mishchenko et al., 1996) using prolate and oblate particles uniformly distributed over all the possible aspect ratios centred around 1 (we found 1% error on SSA and extinction coefficient). Mishchenko et al. (1996) suggested that this phenomenon can occur when large numbers of randomly orientated particles in the sampling chamber are averaged, leading to a smaller error than for individual particle counting. It may be also due to the uncertainties in our measurements, especially of size distribution, and the lack of knowledge on dust morphology. Hence, we have used Mie theory for spherical aerosols in the manuscript. A short paragraph containing the above information has been added to the manuscript.

4. *Aerosol back-scatter to extinction ratio (BER) is assumed constant with altitude. Error in dust radiative forcing resulting from this assumption needs to be presented.* Figure 1a shows the heating profiles associated with constant BER value of 0.02 sr^{-1} (black

solid line) and a BER profile increasing from 0.016 (at the surface) to 0.024 sr^{-1} (at 7 km) (red solid line). Figure 1b shows the uncertainty on the heating rate profile associated the BER profile evolving with altitude (red solid line) and that associated with constant BER profiles (0.016 and 0.04 sr^{-1}, solid line and dash-dotted line, respectively). The former assumption leads to an uncertainty on the heating rate less than 0.5 K day^{-1} and **more importantly smaller than the one associated with the constant BER profiles** (Fig. 1b). In this paper, we discuss the maximum uncertainty associated with the errors on the variables likely to impact the heating rate profiles. Hence, we only discuss the uncertainty associated the BER value of 0.016 sr^{-1}.

(a) (b)

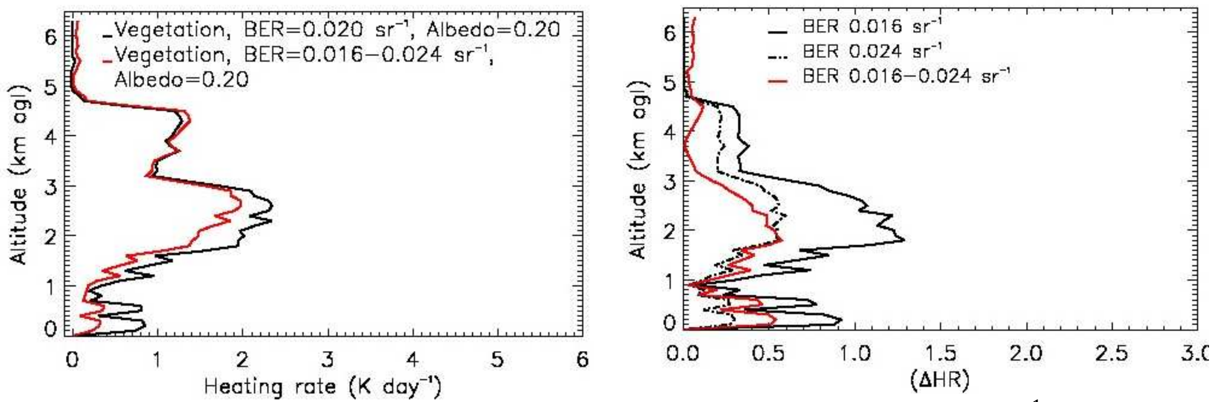

Figure 1: (a) Heating profiles associated with constant BER value of 0.02 sr^{-1} (black solid line) and a BER profile increasing from 0.016 (at the surface) to 0.024 sr^{-1} (at 7 km) (red solid line). (b) Uncertainty on the heating rate profile associated the BER profile evolving with altitude (red solid line) and that associated with constant BER profiles (0.016 and 0.04 sr^{-1}, solid line and dash-dotted line, respectively).

5. *BER is also assumed wavelength independent BER. Please justify these two assumptions.* We have clarified these aspects in the revised bversion. The BER is not assumed wavelength independent. BER has been calculated at the lidar wavelength for both LEANDRE and CALIOP instruments following the climatology given by Omar et al., (2009). In all cases, we used constant profiles of BER with the values corresponding to the desert dust climatology used for CALIOP (described in Omar et al, (2009) interpolated at 730nm for airborne lidar and at 532 nm for CALIOP. However, differences in the multiple scattering effects between the airborne and spaceborne lidars are accounted for through the so-called multiple scattering coefficient η. We neglect these effects when analysing data from the LEANDRE system (η=1) and we use a η profile obtained from MonteCarlo simulations (Young et al., 2008) for CALIOP. This discussion is now included in the manuscript as:

In section 2.2

" LEANDRE-derived aerosol extinction coefficient (AEC) profiles (at 730 nm) were obtained from the total attenuated backscatter coefficient (TABC) profiles, via a standard lidar inversion technique (Fernald et al., 1972; Fernald et al., 1984), with a vertical resolution of 15 m and a horizontal resolution of roughly 500 m. This inversion technique relies on the proportionality of the aerosol backscatter coefficient (ABC) and AEC, i.e. ABC (z)= BER x AEC (z), BER being the aerosol backscatter-to-extinction ratio and z the altitude. We considered that BER is constant with altitude (e.g.; Welton et al., 2000) and we used a value of 0.02 sr-1, which is a climatological value for dust (Omar et al., 2009) interpolated linearly at 730 nm between values provided at 532 nm (0.024 sr-1) and 1064 nm (0.018 sr-1). The molecular backscatter coefficient profiles used in the inversion procedure were obtained from dropsonde-derived pressure and temperature measurements. In the lidar inversion, multiple scattering effects may be considered by introducing a so-called multiple scattering factor η (0≤ η ≤ 1) to account for the reduction of the effective aerosol extinction coefficient η AEC(z) (e.g., Nicolas et al., 1997). In the case of dust particles, this effect can be neglected (η≈1) for airborne lidar measurements (Ackermann et al., 1999) since the volume of air sampled by the lidar beam is sufficiently small (note that the laser footprint on the ground is ~3.5 m wide). Because of the uncertainties on the value of the BER, the sensitivity of dust-related heating rates will be conducted thereafter (see Section 5)."

In section 2.3

"CALIOP-derived aerosol extinction coefficient (AEC at 532 nm) profiles were obtained from our own calculation (using level 1B version 2), with a vertical resolution of 60 m and a horizontal resolution of roughly 12 km. To obtain AEC from TABC profiles, we use the same lidar inversion technique as for LEANDRE 2. The molecular backscatter coefficient profiles used in the inversion procedure were obtained from molecular density profiles extracted from the National Centers for Environmental predictions (NCEP) analyses along CALIPSO tracks. We use a constant BER profile at 532 nm with a value of 0.024 sr^{-1} (Omar et al., 2009). Since CALIOP samples a sufficiently large volume of air (the footprint at the ground is 90 m wide), we considered here a multiple scattering coefficient η for dust particles below one. Following the MonteCarlo simulations of Young et al., (2008) and Berthier et al., (2006), we used a η profile increasing exponentially from 0.65 at the layer top, 0.87 below 500 m above ground level (a.g.l.) and to 0.95 at the ground, as in Cuesta et al. (2009) and Messager et al. (2010)"

6. *Several instruments (Aethalometer from Magee Scientific for example) are designed for ground-based measurements. As a response to changes in pressure at different altitudes, flow through these instruments can vary. Please describe these effects and corrections applied.*: Only data collected during straight and levelled runs at constant altitudes (i.e. pressure) were considered. In particular, the data used in this paper were collected whilst the aircraft was flying at constant altitude at 700 msl, that is, very close to the ground. Over the two entire straight and levelled runs considered in this paper the air flow through the instrument was 11.3 ± 0.4 L min^{-1} (mean ± standard deviation, 13 June) and 10.7 ± 0.1 L min^{-1} (mean ± standard deviation, 14 June). This variability has been taken into account when estimating the errors affecting the measurements.

7. *Various correction factors applied to absorption and scattering coefficients may be provided*: As stated in the paper, corrections factors applied to the scattering and the backscattering coefficients are those described in the publication by Anderson and Ogren, 1998. Corrections factors applied to the absorption coefficient are those described in Weingartner et al., 2003.

8. *Section-2.2.1: It appears that lidar inversion used in LEANDRE-2 lidar (section-2.1) assumes altitude independent BER and CALIOP inversion (section-2.2.1) uses altitude*

dependent BER. If so, please justify. This point is detail in the response to comment #5.

9. *Section-2.3.1: Was there any surface reflectance measurements from aircrafts? Surface reflectance is a vital parameter while assessing radiative forcing especially in bright surfaces like deserts. Uncertainty in MODIS surface albedo product can lead to errors in the estimated dust forcing.* There are no direct surface reflectance measurements available from the aircraft. MODIS provides the best product we can use here. However, we analyze the impact of significant errors on the MODIS albedo on the heating rate values. An error of 60% on surface albedo (0.20 to 0.15 or 0.20 to 0.25) leads to an absolute error lower than 0.2 $Kday^{-1}$ on the heating rate. Moreover as shown in Figure 2 which quantified the surface albedo obtained with MODIS data (in red), using downward and upward visible irradiance obtained along Falcon 20 track (black line), and streamer irradiances (diamond) MODIS albedo is in a good agreement with airborne observations.

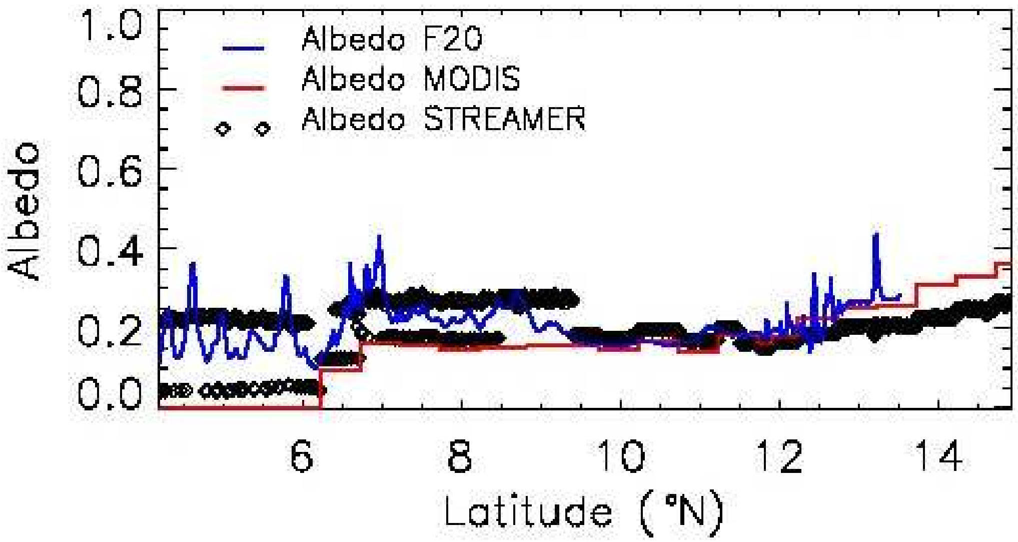

Figure 2: Surface shortwave albedo from MODIS (red line) derived along the F/F20 flight track on 14 June 2006. Superimposed are the total effective albedo (accounting for the surface, aerosol and clouds) obtained from shortwave downwelling and upwelling airborne irradiances (blue line) and from STREAMER-simulated irradiances (dark diamonds).

10. *Section-5: Investigations as part of Aerosol Characterization Experiment-Asia (ACE-Asia) have shown that the dust we observe may not be just dust, but it may be dust mixed with other aerosols. Dust particles mixed with soot, sulfates, nitrates or aqueous solutions can have drastically different properties. I understand that information on aerosol state of mixing, though vital, is not at all discussed in this study. Was there any Scanning Electron Microscope analysis of aerosol samples? I suggest that authors may address this aspect.*: The referee is right. Unfortunately these kinds of measurement are not available during the experiment. However, the investigation of the elemental composition north of 10°N when the ATR-42 was flying in the dust plume show that elements other than typical dust constituents were always lower than detection limits, indicating that mixing is unlikely. Also see the answer to comment #2.

11. *Section-5.1: Considering the fact that a number of assumptions are involved in the assessment of dust radiative forcing, I feel that section 5.1 (sensitivity studies) is too short. Authors may provide a detailed sensitivity analysis and come up with an overall uncertainty in the dust forcing.* In the revised version of the manuscript, we have added a discussion on the overall uncertainty on the dust forcing. The total uncertainty on the HR values, taken as the sum of the quadratic errors related to the type of soil, the albedo, the BER and the extinction, can be written as:

$$\sigma_{\Delta HR} = \sqrt{\left(HR_{alb}0.15 - HR_{alb}0.20\right)^2 + \left(HR_{BER_0}.020\pm0.004 - HR_{BER_0}.020\right)^2 + \left(HR_{ext} - HR_{ext_{10}}\right)^2 + \left(HR_{dry} - HR_{vegeted}\right)^2}$$

In all cases, the total uncertainty is computed with respect to the reference profile.

12. *No validation for dust forcing is presented. Do you have data from upward and downward looking radiometer at least from one flight? If so, it is possible to validate the estimated dust forcing.:* A new section called "**Comparison of irradiances and surface/cloud albedo from the model with measurements**" has been incorporated to presented a validation of longwave & shortwave, upwelling/downwelling irradiances associated with dust and simulated with STREAMER. Comparison is made with surface radiometer measurements (in Wankam, Niger) and onboard the Falcon 20. The following Figure as been to the paper.

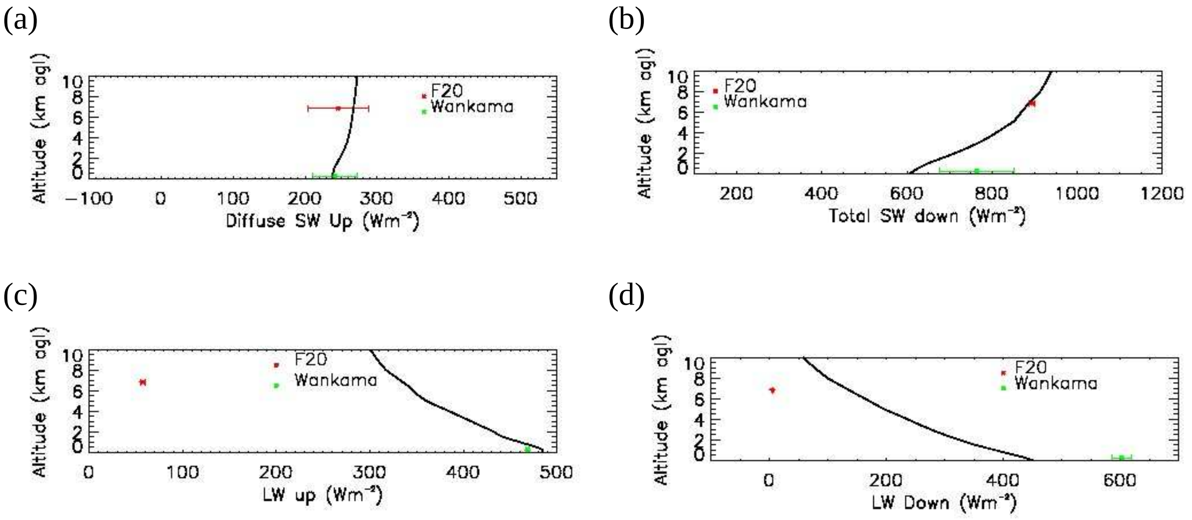

Figure 3*:* Comparison between irradiances profiles derived from STREAMER (black solid line) obtained at the location of the Wankama station and at the time of the F/F20 overpass on 14 June. The data from the F/F20 are in red and data from the Wankama station are in green: upward shortwave **(a)** downward shortwave **(b)**, upward longwave **(c)** and downward longwave **(d)**.

13. In the original version of the paper, we have discussed the importance of the infrared part of the spectrum (0.7-400 µm) to the heating rate. In the revised version of the manuscript, because we are comparing irradiance profiles with radiometry measurements in the longwave and shortwave domain, we have modified our approach to the discussion on the contribution of infrared/visible to the total heating

rate retrievals. We are now considering the shortwave/longwave domains rather than the visible/infrared domains. This when we are also more in line with previpus studies which have attempt to address the partition between longwave and shortwave rather than infrared/visible. In the revised version of the manuscript, we consider the longwave domain to extend from 4 to 400 µm. The following Figure has been added (which replaces the previous one), together with a discussion.

(a)

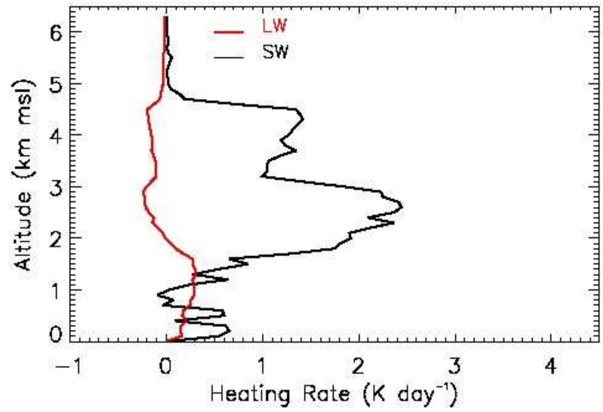

(b)

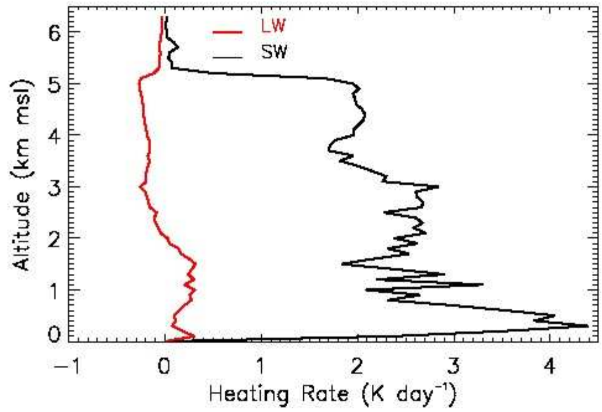

(c)

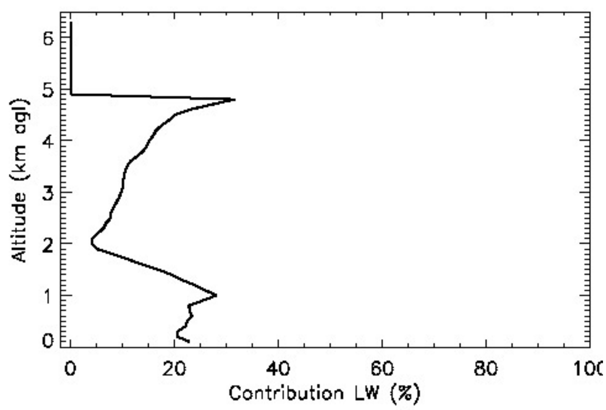

Figure 3 : Heating rate profiles in the longwave domain (red solid line) and in the shortwave domain (black solid line) derived from LEANDRE 2 at 10°N (a) and 13°N (b) with the RaCH model. (c) Relative contribution of the longwave to the total heating rate averaged along the entire F/F20 transect on 14 June.

References (added in the revised version of the manuscript)

Cuesta, J., Edouart, D., Mimouni, M., Flamant, P. H., Loth, C., Gibert, F., Marnas, F., Bouklila, A., Kharef, M., Ouchene, B., Kadi, M., and Flamant, C.: Multi-platform observations of the seasonal evolution of the Saharan atmospheric boundary layer in Tamanrasset, Algeria, in the framework of the African Monsoon Multidisciplinary Analysis field campaign conducted in 2006, J. Geophys. Res., 113, D00C07, 2008.

Collins, D. R., Jonsson, H. H., Seinfeld, J. H., Flagan, R. C., Gasso, S., Hegg, D. A., Schmid, B., Russell, P. B., Livingston, J. M., Ostro E., Noone, K. J., Russell, L. M. and Putaud, J. P.: In situ aerosol size distributions and clear column radiative closure during ACE-2. T ellus 52B, 498–525, 2000.

Dunion, J.P., and C.S. Velden: The impact of the Saharan air layer on Atlantic tropical cyclone activity, BAMS, pp 353-365,doi :10.117/BAMS-85-3-353, 2004.

Evan, A.T., Dunion, J., Foley, J.A., Heidinger, A.K., Velden, C.S.: New evidence for a relationship between Atlantic tropical cyclone activity and African dust outbreaks, Geoph. Res. Letters, 33, L19813, 2006.

Liu, Z., et al.: CALIPSO lidar observations of the optical properties of Saharan dust: A case study of long-range transport, J. Geophys. Res., 113, D07207, doi:10.1029/2007JD008878., 2008.

Mishchenko, M. I., Travis, L. D., and Macke, A.: Scattering of light by polydisperse, randomly oriented, finite circular cylinders, Appl. Opt., 35, 4927–4940, 1996.

Nicolas, F., Bissonnette, L. R. and Flamant, P. H.: Lidar effective multiple-scattering coefficients in cirrus clouds. Appl. Opt. 36, 3458-3468, 1997.

Omar, A.H., Winker, D., Kittaka, C., Vaughan, M.A., Liu, Z., Hu, Y., Trpte, C.R., Rogers, R.R, Ferrare, R.A., Lee, K-P., Kuehn, R.E. and Hostetler, A.: The CALIPSO Automated Aerosol Classification and Lidar Ratio Selection Algorithm, J. of Atm. and Oceanic Technology, 26, 1994-2014, 2009.

Roman, M., Schaaf, C.B., Lewis, P., Gao, F., Anderson, G.P., Privette, J.L., Strahler, A.H., Woodcock, C.E., Barnsley, M.: Assessing the coupling between surface albedo derived from MODIS and the fraction of diffuse skylight over spatially- characterized landscapes, Remote Sensing of Environment, 114, 738–760, 2010.

Wandingern U., Tesche, M., Seifert, P., Ansmann, A.: Size matters: Influence of multiple scattering on CALIPSO light-extinction profiling in desert dust, Geophysical Research Letters, 37, L10801, 5 PP., doi:10.1029/2010GL042815, 2010.

Weinzierl, B., Petzold, A., Esselborn, M., Minikin, A. Fix, A., Wirth, M. and Fiebig, M. : The Airborne Aerosol Measurements During SAMUM-1 and SAMUM-2 : What Have we Learned About Dust ?, AGU Fall Meeting 2008, San Francisco, CA (USA), 15-19 December 2008, A41K-08, 2008.

Winker, D. M., Vaughan, M.A, Omar, A., Hu, Y., Powell, K.A., Liu, Z., Hunt, H.W., and Young, S.A. : Overview of the CALIPSO mission and CALIOP data processing algorithms, J. Atmos. Oceanic Technol., 26, 2310–2323.